Ann. Geophys., 40, 531–544, 2022
https://doi.org/10.5194/angeo-40-531-2022
© Author(s) 2022. This work is distributed under
the Creative Commons Attribution 4.0 License.

Annales Geophysicae Open Access EGU

Multiple conjugate observations of magnetospheric fast flow bursts using THEMIS observations

Homayon Aryan[1], **Jacob Bortnik**[1], **Jinxing Li**[1], **James Michael Weygand**[2], **Xiangning Chu**[3], **and Vassilis Angelopoulos**[2]

[1]University of California Los Angeles, Atmospheric and Oceanic Sciences, Math Sciences Building, Los Angeles, California 90095-1565, USA
[2]Department of Earth, Planetary and Space Sciences, University of California Los Angeles, California 90095, USA
[3]Laboratory for Atmospheric and Space Physics, University of Colorado, Boulder, Colorado 80303, USA

Correspondence: Homayon Aryan (aryan.homayon@gmail.com)

Received: 20 January 2022 – Discussion started: 26 January 2022
Revised: 12 May 2022 – Accepted: 14 June 2022 – Published: 5 August 2022

Abstract. Magnetotail earthward fast flow bursts can transport most magnetic flux and energy into the inner magnetosphere. These fast flow bursts are generally an order of magnitude higher than the typical convection speeds that are azimuthally localised (1–3 R_E) and are flanked by plasma vortices, which map to ionospheric plasma vortices of the same sense of rotation. This study uses a multipoint analysis of conjugate magnetospheric and ionospheric observations to investigate the magnetospheric and ionospheric responses to fast flow bursts that are associated with both substorms and pseudobreakups. We study in detail what properties control the differences in the magnetosphere–ionosphere responses between substorm fast flow bursts and pseudobreakup events, and how these differences lead to different ionospheric responses. The fast flow bursts and pseudobreakup events were observed by the Time History of Events and Macroscale Interaction during Substorms (THEMIS), while the primary ionospheric observations were made by all-sky cameras and magnetometer-based equivalent ionospheric currents. These events were selected when the satellites were at least 6 R_E from the Earth in radial distance and a magnetic local time (MLT) region of ± 5 h from local midnight. The results show that the magnetosphere and ionosphere responses to substorm fast flow bursts are much stronger and more structured compared to pseudobreakups, which are more likely to be localised, transient and weak in the magnetosphere. The magnetic flux in the tail is much stronger for strong substorms and much weaker for pseudobreakup events. The B_{lobe} decreases significantly for substorm fast flow bursts compared to pseudobreakup events. The curvature force density for pseudobreakups are much smaller than substorm fast flow events, indicating that the pseudobreakups may not be able to penetrate deep into the inner magnetosphere. This association can help us study the properties and activity of the magnetospheric earthward flow vortices from ground data.

1 Introduction

Magnetic reconnection in the Earth's magnetosphere converts open magnetic flux in the lobes into closed magnetic flux in the plasmasheet. A magnetospheric substorm is an important energy unloading process in the magnetosphere. This process converts lobe magnetic energy into the thermal and kinetic energy of fast flow bursts, which are also known as bursty bulk flows (BBFs) in the central plasmasheet (Hones Jr. et al., 1970; McPherron, 1970; McPherron et al., 1973; Baker, 1996; Angelopoulos et al., 1992; Angelopoulos et al., 2008). These processes may repeat many times in the course of a moderate to strong substorm (Sergeev et al., 2014). These bursty bulk flows are an important component of plasmasheet dynamics during many different geomagnetic activity conditions. They are a common feature of radial transport throughout the plasmasheet and typically are associated with magnetic field dipolarisations (Nakamura et al., 2002) and plasmasheet heating (Runov et al., 2015). They are observed on short timescales of around minutes and small-scale sizes of a few Earth radius (R_E) in the X and Y directions

(Gabrielse et al., 2019; Liu et al., 2013b). They exhibit large earthward velocities that are usually an order of magnitude higher than the typical convection speeds, and transport magnetic flux and energy into the inner magnetosphere that often decelerate and stop at around 8–10 R_E (Angelopoulos et al., 1992; McPherron et al., 2011; Hsu and McPherron, 2012; Runov et al., 2014; Sergeev et al., 2014; Liu et al., 2014). The rebound of earthward fast flow bursts can also cause a tailward fast flow (Nakamura et al., 2009; Birn et al., 2011). Even though substorms are closely associated with fast flow bursts generated by magnetic reconnection in the tail (Liu et al., 2013a; Liu et al., 2015), not all fast flow bursts are necessarily associated with a global response (e.g. McPherron et al., 2011; McPherron and Chu, 2018; Chu et al., 2015b) and they can also form spontaneously (Sitnov et al., 2013). It was shown that the strength of a substorm is related to the magnetic flux accumulated in the inner magnetosphere (Chu et al., 2021). Furthermore, the midlatitude positive bay (MPB) index is used to distinguish the difference between global substorms and pseudobreakups (Chu et al., 2015a). It is insensitive to the localised fine structure of the electrojet and can capture the global substorm current wedge well. Using a list of global substorms and pseudobreakups, it was found that substorm-onset-related fast flows are associated with stronger dipolarisations in Bz and larger magnetic flux transport rates than non-substorm fast flows (Li et al., 2021). Many fast flow bursts are associated with localised, transient and weak responses in the magnetosphere and ionosphere (Li et al., 2021), and may not involve auroral brightening (Nishimura et al., 2011) or plasmasheet injections (narrow high-speed flow bursts that were initially studied in detail as a substorm phenomenon (Baker et al., 1982; Baker, 1996; Lopez et al., 1990; McIlwain, 1972) at a geosynchronous orbit (GEO) due to the availability of many satellite observations in this region) (Akasofu, 1964; Birn et al., 1997). However, substorm fast flow bursts are more likely to penetrate closer to the Earth and are typically accompanied by a larger magnetic field increase and magnetic field energy input than non-substorm fast flow bursts (Li et al., 2021).

The magnetospheric substorm disturbances are associated with the formation of the substorm current wedge (SCW) (Birn and Hesse, 2014; Kepko et al., 2014; Kepko et al., 2015; McPherron, 1979) that electrically couples the near-Earth plasmasheet with the ionosphere through at least one pair of downward and upward field-aligned currents (FACs) (Liu et al., 2013a; Sun et al., 2013). The pressure gradient of current and inertial current are thought to be the sources of the SCW (Yao et al., 2012; Birn and Hesse, 2013), both of which are perpendicular currents and are believed to be diverted to form the field-aligned portion of the SCW (Keiling et al., 2009). The field-aligned currents within the ionosphere are connected to one another via mostly Pedersen currents. The westward electrojet and eastward electrojet are mostly Hall currents that are believed to be anti-parallel to the ionospheric convection. The auroral brightening associated with substorm onset is the deposition of electrons into the ionosphere (Akasofu, 1964; McPherron et al., 1973; Lyons et al., 2012), typically associated with the upward field-aligned current as the magnetic field lines become more depolarised and the SCW intensifies (Chu et al., 2015b).

The magnetosphere–ionosphere responses between substorm and non-substorm (pseudobreakups) events have been studied in the past (e.g. Ohtani et al., 1993; Koskinen et al., 1993; Nakamura et al., 1994; Baumjohann et al., 1989; Baumjohann et al., 2010). They have concluded that substorms and pseudobreakups have common responses (e.g. fast flows, dipolarisations, injections, electrojet and current wedge) without phenomenological differences. The differences between substorms and pseudobreakups are thought to be the strength, scale size and duration of activity; substorms have stronger and global activity, but non-substorm conditions have weaker and localised activity. It has been shown that the substorm–time ionospheric currents have clockwise and counter-clockwise vortices (Keiling et al., 2009) that are connected to plasma flow vortices in the magnetosphere (Akasofu, 1976; Borovsky and Bonnell, 2001). However, there is limited direct observational evidence of this connection, largely due to the difficulty of finding conjunctions. Keiling et al. (2009) performed a multipoint analysis of conjugate magnetospheric and ionospheric flow vortices for a single substorm-related fast flow bursts to show that the equivalent ionospheric current (EIC) vortices were directly driven by the vortices observed in the magnetosphere. This study uses a multipoint analysis of conjugate magnetospheric and ionospheric observations to investigate the magnetospheric and ionospheric responses to fast flow bursts that are associated with both substorms and pseudobreakups. In this study, we look into what properties control the differences in the magnetosphere–ionosphere responses between substorm fast flows and pseudobreakup events, and how these differences lead to different ionospheric responses. We analyse the Time History of Events and Macroscale Interaction during Substorms (THEMIS) observations and the all-sky imager (ASI) data on the ground. We then select three pairs of fast flow and pseudobreakup events that were observed by all three inner THEMIS satellites (THEMIS A, D and E) on the nightside, and study their properties.

2 Data

The THEMIS mission (Angelopoulos, 2008) was launched in February 2007 and consists of five identically equipped satellites (A, B, C, D and E). The main goal of this mission is to carry out multipoint investigations of substorm phenomena in the tail of the terrestrial magnetosphere (Sibeck and Angelopoulos, 2008). The fluxgate magnetometer (MAG) measures the background magnetic field (Auster et al., 2008). The electric field instrument (EFI) (Bonnell et al., 2008) measures the wave electric field. The electrostatic analyser

(ESA) measures the thermal (5 eV–25 keV) ions and electrons (McFadden et al., 2008). The solid state telescope (SST) measures the hot (25 keV to > 1 MeV) ions and electrons (Angelopoulos et al., 2008). In this study, observations from the three inner probes (A, D and E) are analysed to identify fast flow bursts that were observed when the three satellites were closely separated on the nightside, located at least 6 R_E away from the Earth in radial distance and within a magnetic local time (MLT) region of ± 5 h from local midnight.

The all-sky imager (ASI) data on the ground are analysed to complement the response of the ionosphere to fast flow bursts. The ground data provide contextual information of the processes observed in space by providing a two-dimensional view of the injection's formation and propagation and its connection to the substorm evolution. A series of ground magnetometer arrays are used to generate the equivalent ionospheric currents (EICs) and current amplitudes at 10 s resolution, using the spherical elementary current systems (SECS) technique (Amm and Viljanen, 1999; Amm et al., 2002; Weygand et al., 2011, 2012; Weygand and Wing, 2016). This consists of a curl-free system whose divergences represent the FACs. It also consists of a divergence-free elementary system that is contained entirely within the ionosphere (Amm et al., 2002). This study analyses the EICs during conjunctions with the THEMIS satellites for the selected fast flow cases.

The electron flux data at a geostationary orbit are measured by the magnetospheric electron detector (MAGED) (Rowland and Weigel, 2012) on board the Geostationary Operational Environmental Satellite (GOES) 13 and 15. The MAGED operates on five energy channels: 40, 75, 150, 275 and 475 keV, and has nine telescopes pointing in different directions.

The substorms are identified using the midlatitude positive bay (MPB) index (McPherron and Chu, 2017) and by checking the SuperMAG auroral electrojet indices (SMU and SML) (Gjerloev, 2009; Newell and Gjerloev, 2011). The MPB index is calculated as the moving variance of changes in the H and D components ($\Delta H^2 + \Delta D^2$), obtained generally from 20 to 53 stations at midlatitudes (20–52° in magnetic latitude) from the International Real-time Magnetic Observatory 127 Network (Chu et al., 2015a).

3 Selection criteria

In this study, we analysed the THEMIS observations to identify fast flow burst events that were observed by all three inner THEMIS satellites (THEMIS A, D and E) at the end of 2015 when the THEMIS configuration was identical to that considered by Sergeev et al. (2012) and was recreated by the THEMIS mission operations team. This unique tail science phase configuration lasted around three months (October, November and December). The configuration of the three THEMIS spacecraft were very favourable for determining the magnetic field gradients and plasma parameters in the magnetotail. This was because the y coordinates of the three satellites were almost the same and it could be assumed that all differences between the magnetic field measured at the three satellites are caused by the satellite separation in the (x, z) plane, allowing us to derive the time-varying parameters, such as the current density, lobe magnetic field, curvature force density and plasma pressure.

We studied the data from this unique tail science phase configuration to identify pairs of fast flows (where one event represented pseudobreakups and another event represented substorm fast flow burst) that occurred within a few hours of each other on the same orbit (so that the background conditions were as similar as possible), during close separation between the three inner THEMIS satellites on the nightside, located at least 6 R_E away from the Earth in radial distance and within a magnetic local time (MLT) region of ± 5 h from local midnight. The MPB index and the auroral electrojet indices were used to distinguish between pseudobreakups (quiet conditions) and substorm (active conditions) fast flow bursts, where the MPB substorm is defined as the MPB index larger than 25 nT^2. The SuperMAG auroral electrojet indices (SMU and SML) were checked and plotted for convenience to show the difference for substorm fast flow bursts and pseudobreakup events. The MPB index is used because it is insensitive to the localised fine structure of the electrojet and can capture the global substorm current wedge well.

In addition, the fast flow bursts were selected based on at least one sample of the perpendicular velocity projected to the XY plane exceeding 150 $km\,s^{-1}$. The start/end time of the fast flow bursts were defined by the first/last time when the earthward velocity component exceeded 120 $km\,s^{-1}$. The observations while the THEMIS satellites were in the eclipse were excluded. Fast flow bursts that occurred within 60 s of each other were merged into one flow (Li et al., 2021). The above criteria allowed us to identify the three pairs of fast flow bursts that are discussed in this study.

4 Observations

The THEMIS spacecraft in situ measurements for six selected fast flow burst cases are shown in Figs. 1–3. The pseudobreakups fast flow bursts are highlighted in green (Cases 1, 3 and 5), while substorm-related fast flow bursts are highlighted in yellow (Cases 2, 4 and 6). Figure 1 shows the pair of fast flow bursts – Cases 1 and 2 – that were observed on 25 December 2015. The pseudobreakups fast flow burst, Case 1, was observed around 05:35 UT by all three THEMIS spacecraft. The MPB index was around 5 nT^2 and all three spacecraft observed magnetic field fluctuations. The Bx magnetic field component decreased by ∼20 nT, while the Bz magnetic field component increased by ∼20 nT. THEMIS D observed the maximum ion perpendicular velocity of around

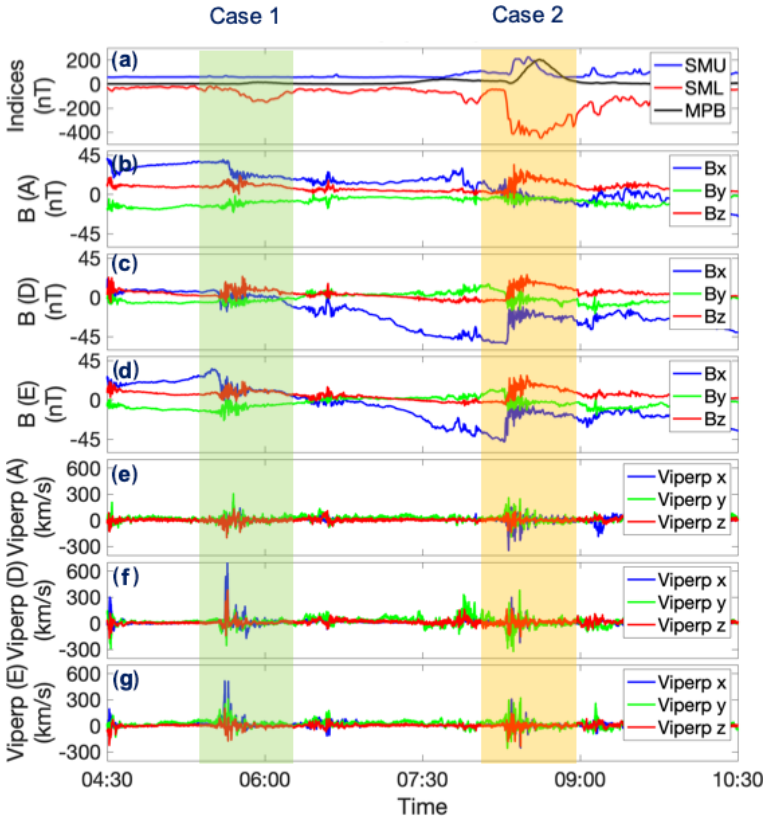

Figure 1. THEMIS spacecraft in situ measurements for fast flow burst Cases 1 and 2 that were observed on 25 December 2015. The pseudobreakup events are highlighted in green (Case 1), while the substorm fast flow burst events are highlighted in yellow (Case 2). **(a)** The auroral electrojet indices SMU, SML and MPB index, **(b–d)** the 3-D magnetic field measured by THEMIS A, D and E, respectively, and **(e–g)** the perpendicular ion velocity measured by THEMIS A, D and E, respectively.

725 km s^{-1} in the x direction. Approximately 2.5 h later, at around 08:17 UT, all three THEMIS spacecraft observed another burst of fast flows, i.e. Case 2. The MPB index increased to just over 200 nT^2 and all three THEMIS spacecraft observed a significant fluctuation in magnetic field and ion perpendicular velocity, which was consistent across all three spacecraft. The Bx and Bz magnetic field components increased, while THEMIS D observed the maximum ion perpendicular velocity of around 310 km s^{-1} in the x direction.

Figure 2 shows the pair of fast flow bursts, Cases 3 and 4, that were observed on 20 December 2015. The pseudobreakups fast flow burst, Case 3, was observed around 02:40 UT by all three THEMIS spacecraft, when the MPB index was around 20 nT^2. All three spacecraft observed fluctuations in magnetic field and ion perpendicular velocity. The peak ion perpendicular velocity of around 290 km s^{-1} was observed by THEMIS A, while all three spacecraft observed an increase in the Bz magnetic field component. On the other hand, the substorm fast flow burst, Case 4, was observed around 2 h later. The MPB index increased to more than 2500 nT^2, indicating a large substorm. All three THEMIS spacecraft observed a significant variation in magnetic field and ion perpendicular velocity. The peak ion perpendicular velocity, around 530 km s^{-1}, was observed by THEMIS E. In addition, Fig. 3 shows the pair of fast flow bursts, Cases 5 and 6, that were observed on 10 December 2015. The pseudobreakups fast flow burst, Case 5, was observed around 06:50 UT when the MPB index was around 10 nT^2. All three THEMIS spacecraft observed fluctuations in magnetic field and ion perpendicular velocity. In this case, THEMIS E observed the largest peak ion velocity of around 600 km s^{-1}. The substorm fast flow burst was observed less than an hour later at around 07:40 UT, as the MPB index increased to around 570 nT^2. Again, the fluctuations in the magnetic field and ion perpendicular velocity were consistently observed by all three THEMIS spacecraft. The Bx magnetic field components decreased, while THEMIS D observed the maximum ion perpendicular velocity of around 500 km s^{-1} in the x direction.

The location of the three THEMIS spacecraft (THEMIS A, D and E) in the GSM coordinate system for the selected fast flow bursts is shown in Fig. 4. The yellow and green dots indicate where each fast flow was observed along the orbit of each THEMIS spacecraft. During the observation of these six fast flow burst events, the configuration of the three THEMIS spacecraft was very favourable for determining the magnetic

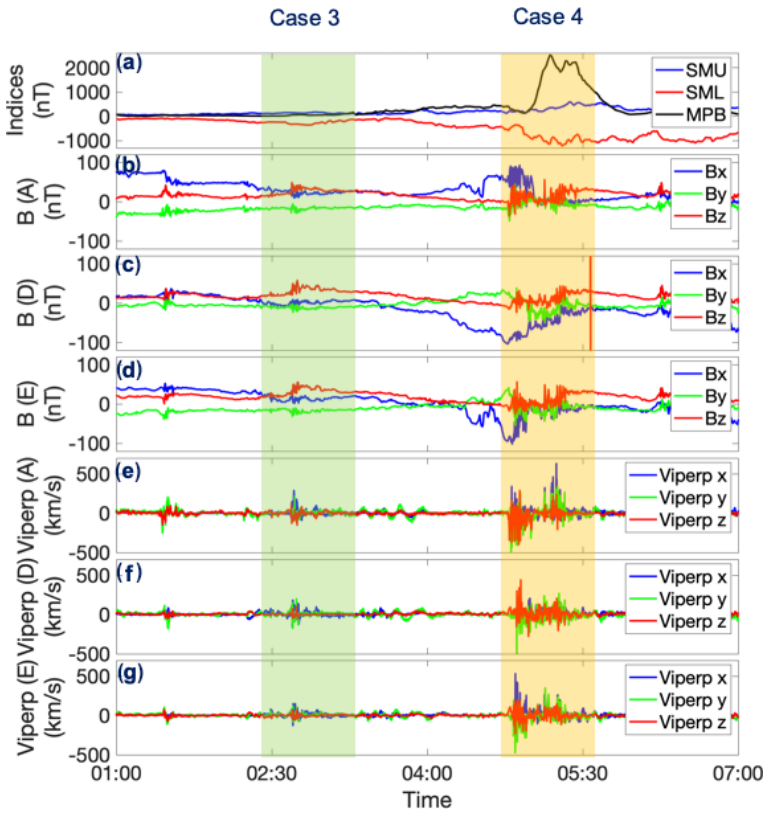

Figure 2. THEMIS spacecraft in situ measurements for fast flow burst Cases 3 and 4 that were observed on 20 December 2015. The caption of Fig. 1 applies.

field gradients and plasma parameters in the magnetotail because the y coordinates of the three satellites were almost the same and it could be assumed that all differences between the magnetic field measured at the three satellites are caused by satellite separation in the (x, z) plane. In the tail science phase (September to December 2015), the apogee of the three THEMIS spacecraft was approximately 12 R_E. The probes were separated by 1000 km to a few Earth radii at apogee. In addition, during the observation of the selected fast flow bursts, at least one of the two GOES 13 and 15 satellites were ideally located on the nightside to observe injections that may have been associated with the earthward fast flow bursts. The next section discusses the derived equivalent ionospheric currents and current amplitudes (the current amplitudes are simply the current perpendicular to the ionosphere at an altitude of 100 km), the ASI data on the ground and the electron flux data from the MAGED measurements on board the GOES 13 and 15 satellites associated with each fast flow burst.

The substorm ionospheric currents are typically accompanied with a clockwise and a counter-clockwise vortex associated with corresponding vortices in the magnetosphere. Multipoint analysis of conjugate magnetospheric and ionospheric flow vortices for a single substorm-related fast flow burst was performed by Keiling et al. (2009) to show that the EIC vortices were directly driven by the flow vortices in the magnetosphere. In this study, we investigate the magnetospheric and ionospheric response to fast flow bursts during both substorm and non-substorm times. We analysed in detail the six fast flow burst cases. Figure 5 shows the derived EICs and their current amplitudes plotted over ASI mosaics for fast flow burst Case 4 that was observed on 20 December 2015. This fast flow burst corresponds to Case 4, which is a substorm-time flow and the THEMIS satellites began observing the flow around 04:50 UT on 20 December 2015 (Fig. 2). Before the initiation of the flow burst, ∼ 04:45 UT (Fig. 5a and b), there were very weak, large-scale clockwise flow vortices that overlapped with the footprint of the THEMIS satellites. The centre of the vortex is located at about 55° Glat and 257° WGLong (marked by green circles). Note that clockwise and counter-clockwise rotations correspond to downward and upward FAC, respectively. At this time there were only downward region 2 and upward region 1 currents. Two thin equatorward drifting east–west auroral arcs, moving south in ASIs WHIT (61°, 225°), FSIM (62°, 239°), FSMI (60°, 248°), and ATHA (55°, 247°) were also observed starting at about 04:45 UT. However, during the fast flow burst event, ∼ 04:50 UT (Fig. 5c and d), relatively stronger counter-clockwise current vortices develop at 52° GLat and 265° WGlong and the downward region 1

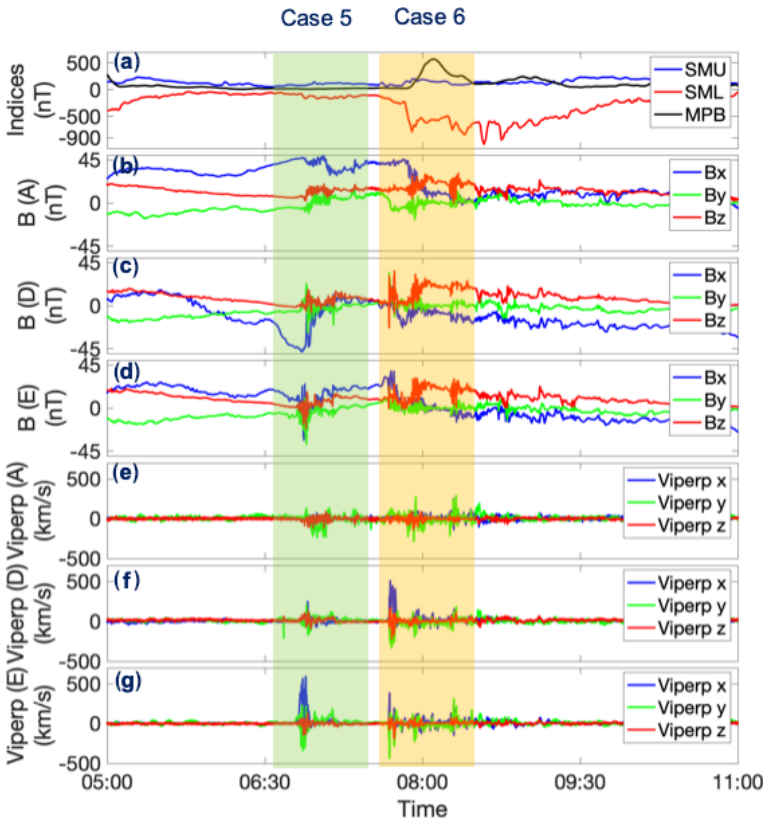

Figure 3. THEMIS spacecraft in situ measurements for fast flow burst Cases 5 and 6 that were observed on 10 December 2015. The caption of Fig. 1 applies.

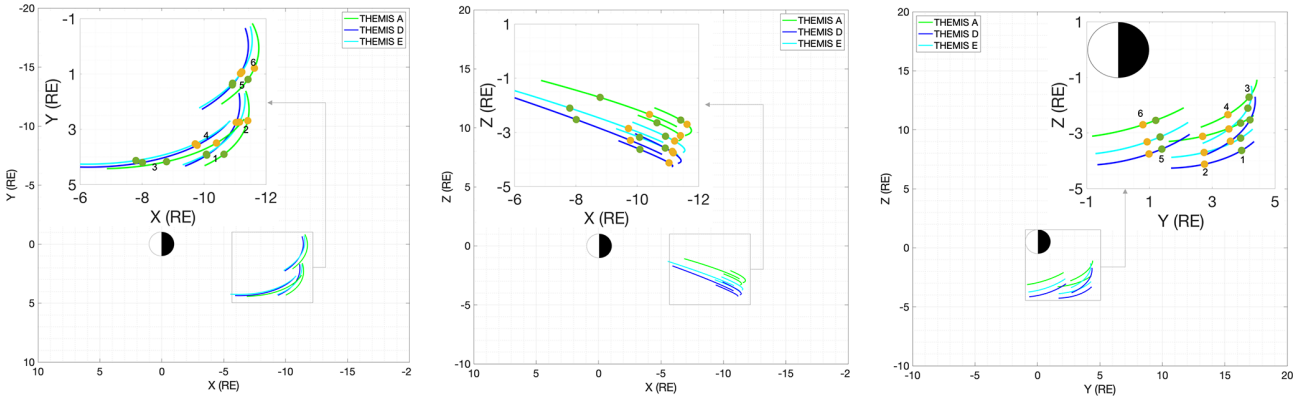

Figure 4. The location of the three THEMIS satellites (THEMIS A, D and E) in the GSM coordinate system for the selected fast flow burst Cases 1–6. The green and yellow dots indicate the exact location where each fast flow burst was observed along the spacecraft orbit.

current system and upward Harang current intensifies just north and south, respectively of the THEMIS satellite foot points. An intensified westward electrojet and the poleward arc formed/brightened in ASIs FSIM and FSMI at about 04:53 UT. The strong current vortices in the equivalent ionospheric currents were continuously observed and intensified to the end of the fast flow burst, ∼ 04:58 UT (Fig. 5e and f). A streamer in ASIs FSMI and ATHA is also observed starting at about 04:53 UT and ending by about 05:02 UT. The equivalent currents closest to the streamer point poleward from about 04:53 to 04:55 UT, then rotates and point toward the SW from 04:57 to 05:02 UT. The aurora brightened at the ATHA ASI from about 04:51 UT and moved poleward into the field of view of the RANK ASI starting at 04:56 UT. These observations are consistent with past observations (Keiling et al., 2009; Li et al., 2021), indicating

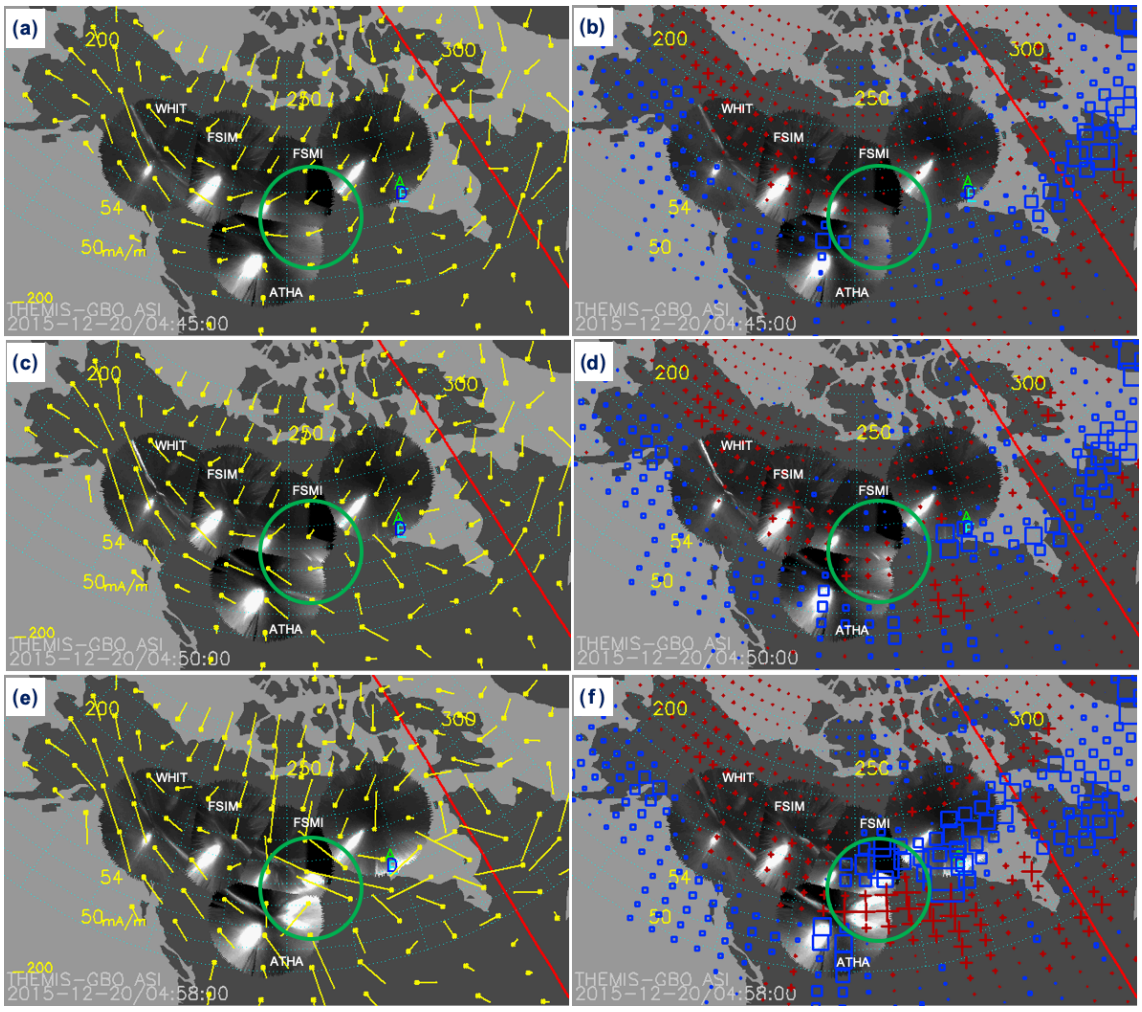

Figure 5. The derived equivalent ionospheric currents and current amplitudes plotted over a sequence of ASI mosaics for fast flow burst Case 4 on 20 December 2015. The yellow arrows represent the direction and the strength of the horizontal currents. The blue squares and the red plus signs show the current amplitudes. The red lines mark the midnight local time. The footprints of the three THEMIS satellites at an altitude of 110 km are marked by letters A (THEMIS A), D (THEMIS D), and E (THEMIS E). Each ASI field of view is approximately 800 km when mapped to a 110 km altitude. The green circles mark the area of discussion. The snapshots show measurements **(a, b)** before, **(c, d)** during, and **(e, f)** after the fast flow burst.

that the ionospheric currents are associated with plasma flow vortices in the magnetosphere for fast flow bursts that are associated with substorms.

The same analysis was performed on pseudobreakups. Figure 6 shows the derived equivalent ionospheric currents and their current amplitudes plotted over a sequence of ASI mosaics for fast flow burst Case 1. This fast flow burst occurred during relatively quiet geomagnetic activity conditions and the inner THEMIS satellites began observing the flow around 05:35 UT on 25 December 2015 (Fig. 1). Before the initiation of this fast flow burst, ∼ 05:30 UT (Fig. 6a and b), the EICs were very weak and the ASIs did not observe significant activity. However, during the fast flow burst, ∼ 05:38 UT (Fig. 6c and d), larger EICs were observed near the satellite foot points. This enhancement in the EICs begins at about 05:37 UT. To west of the spacecraft foot points the EICs point southward and to the east of the footpoints the EICs point poleward indicating the foot points are within the Harang current system. The EICs continued to strengthen to the end of the fast flow burst, ∼ 05:50 UT (Fig. 6e and f). During the fast flow burst the spacecraft foot points were located in the upward (red) Harang current and between a downward region 1 current system and a downward region 2 current system. Starting at 05:49 UT an auroral streamer appears between the downward and upward currents, consistent with the magnetospheric fast flow burst (Kauristie et al., 2000; Nakamura et al., 2001, 2004). Figure 6e shows a streamer was present in both the GILL (56° 265°) and RANK (63° 268°) ASIs between 05:49 and 05:51 UT, but the poleward pointing EICs suggest that the streamer is present

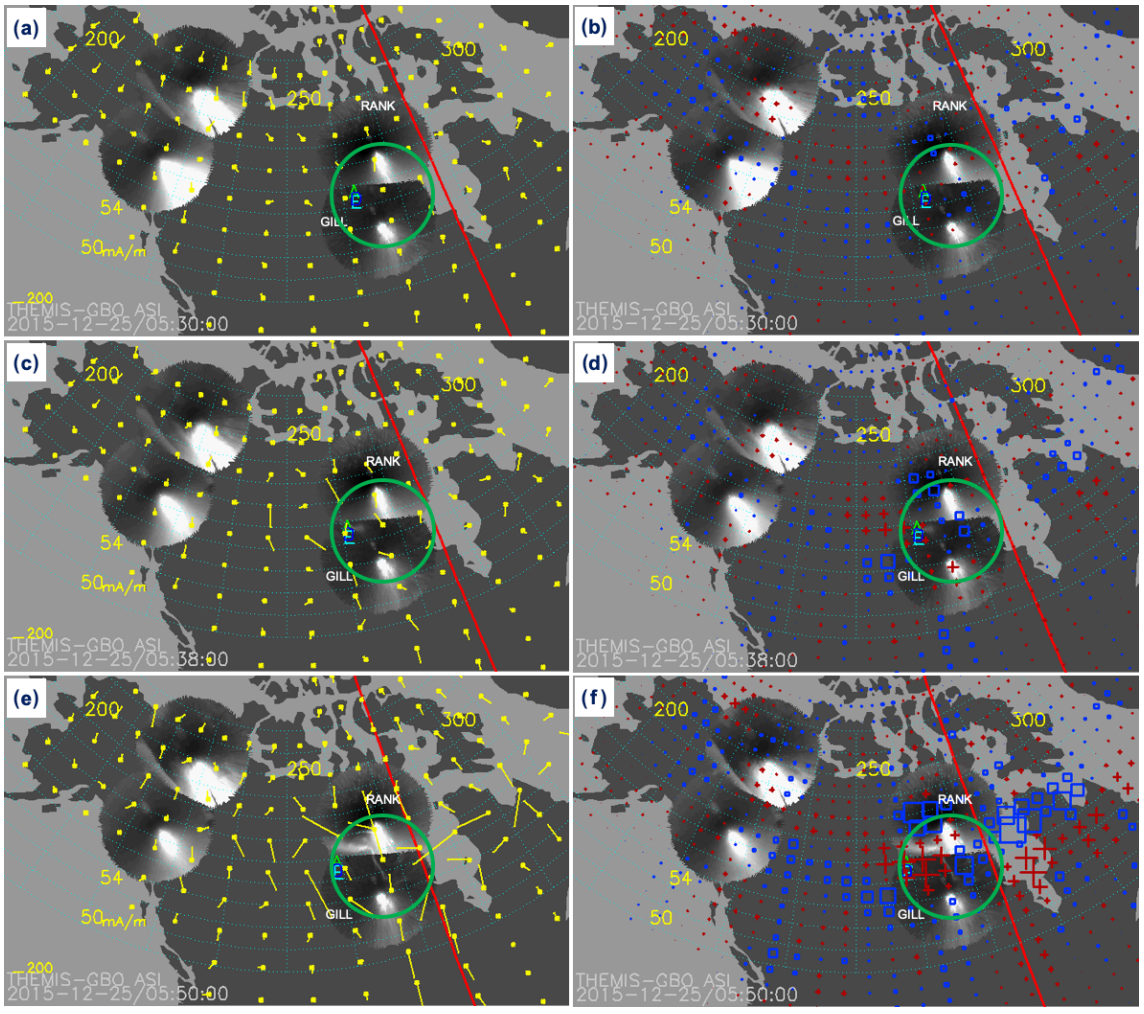

Figure 6. The derived equivalent ionospheric currents and current amplitudes plotted over a sequence of ASI mosaics for fast flow burst Case 1 on 25 December 2015. The caption of Fig. 2 applies.

until about 05:57 UT (marked by green circles). The EICs just to the east of the streamer pointed poleward, which is a good indicator of ionospheric flow from the north to the south and consistent with a north–south streamer. The current density near the foot point of the THEMIS spacecraft just prior to the fast flow burst at 05:35 UT had current density of about 0.1 $\mu A\,m^{-2}$ and increased to a peak value of 1 $\mu A\,m^{-2}$ near the end of the flow burst. This shows that although the ionosphere current response to the pseudobreakups is not as strong as it is for substorm fast flow bursts, nevertheless it is still connected to plasma flow vortices in the magnetosphere.

The earthward fast flow bursts could also play an important role in actively accelerating particles or directly injecting energetic particles into the inner magnetosphere. At substorm onset, the particle flux increases and often lasts tens of minutes to over an hour. In this study, we analyse the electron flux data from the MAGED observations on board the GOES 13 and 15 satellites. These two satellites were ideally positioned on the nightside to observe such injections for the selected fast flow burst cases.

The magnetosphere response to pseudobreakups, Case 1, at around 05:35 UT on 25 December 2015 is presented in Fig. 7. The magnetic field measured by THEMIS A, D and E, respectively, is shown in Fig. 7a–c, while the perpendicular ion velocity measured by THEMIS A, D and E, respectively, is shown in Fig. 7d–f, and the magnetic field from GOES 13 and GOES 15 is shown in Fig. 7i and j, respectively. Figure 7k and l show the electron flux measured by GOES 13 and GOES 15, respectively. The grey vertical lines mark the peak perpendicular velocity associated with each fast flow burst as observed by each THEMIS spacecraft. It is clear that both GOES 13 and GOES 15 satellites did not observe significant flux increase for any of the five energy channels (40, 75, 150, 275 and 475 keV). Also, both GOES 13 and GOES 15 did not observe any significant variation in the magnetic field. For this particular case, both GOES 13 and GOES 15 space-

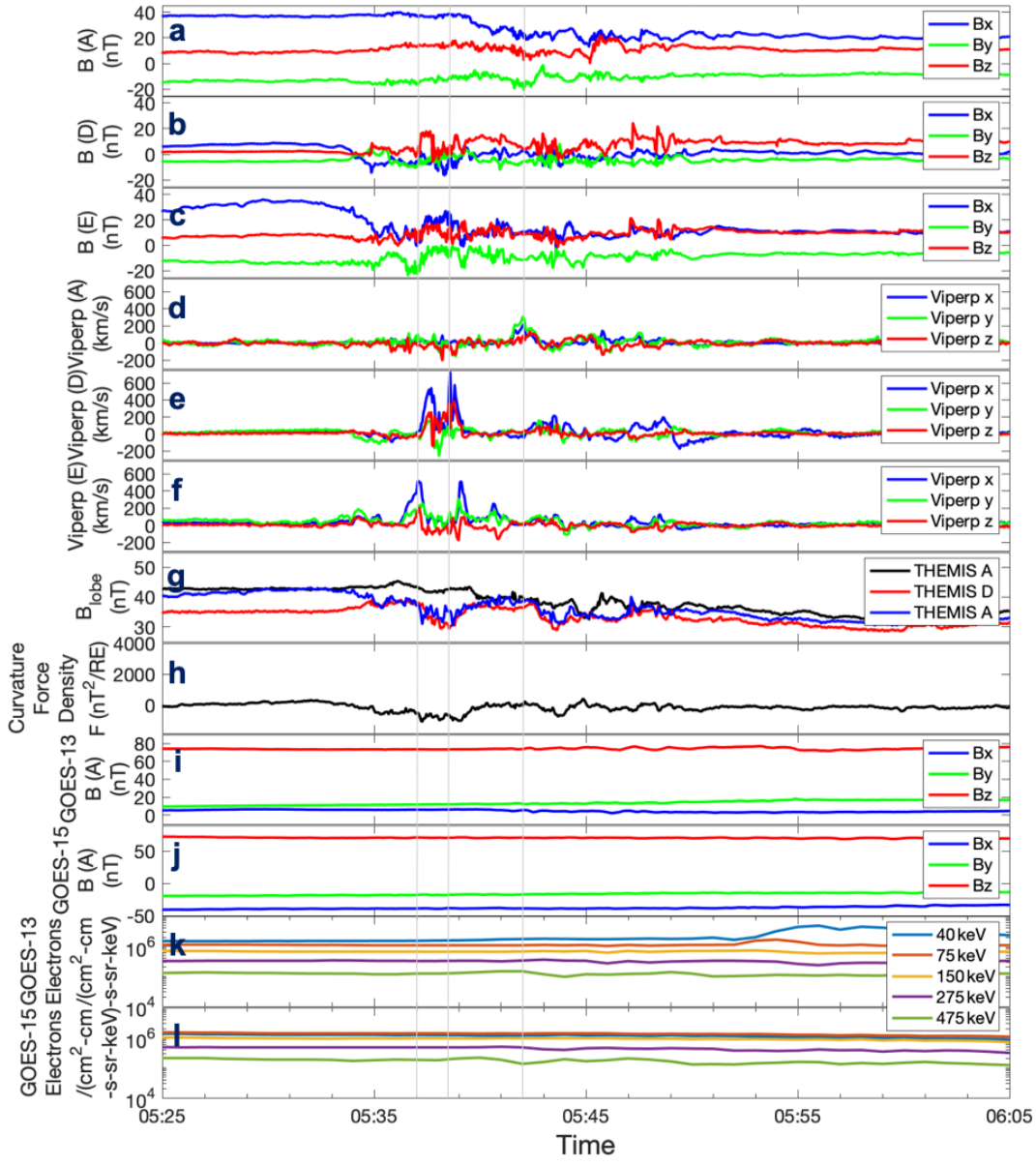

Figure 7. THEMIS spacecraft in situ measurements for pseudobreakup Case 1 on 25 December 2015. **(a–c)** The magnetic field measured by THEMIS A, D and E, respectively, **(d–f)** the perpendicular ion velocity measured by THEMIS A, D and E, respectively, **(g)** the magnetic lobe (B_{lobe}), **(h)** the curvature force density (F), **(i, j)** the magnetic field from GOES 13 and GOES 15, respectively, **(k)** electron flux measured by GOES 13 and **(l)** electron flux measured by GOES 15. The grey vertical lines mark the location of peak perpendicular ion velocity observed by each satellite associated with the fast flow bursts.

craft were located on the nightside, around 6 R_{E} away from the THEMIS spacecraft at around 0.5 MLT and 21 MLT, respectively. The GOES 13 spacecraft was located slightly to the dawn-side, around 2 h MLT from the THEMIS spacecraft, and may have not been able to observe injections related to the fast flow burst. However, the GOES 15 spacecraft was within 1 h MLT from the three THEMIS spacecraft and ideally located to observe injections associated with the fast flow burst, but did not observe anything. This is an indication that pseudobreakups may only cause localised particle injections that do not penetrate very deep into the magnetosphere and, hence, are not observed at geosynchronous orbit. The same can be shown for the other two pseudobreakup cases (Case 3 and 5) presented in this study.

Figure 8 shows the magnetosphere response to substorm fast flow bursts, Case 2, at around 08:17 UT on 25 December 2015. Clearly, both GOES 13 and GOES 15 observed significant flux increases in multiple energy channels. In this case, the GOES 15 spacecraft was within the same MLT hour (∼23 MLT). GOES 15 began observing a flux increase

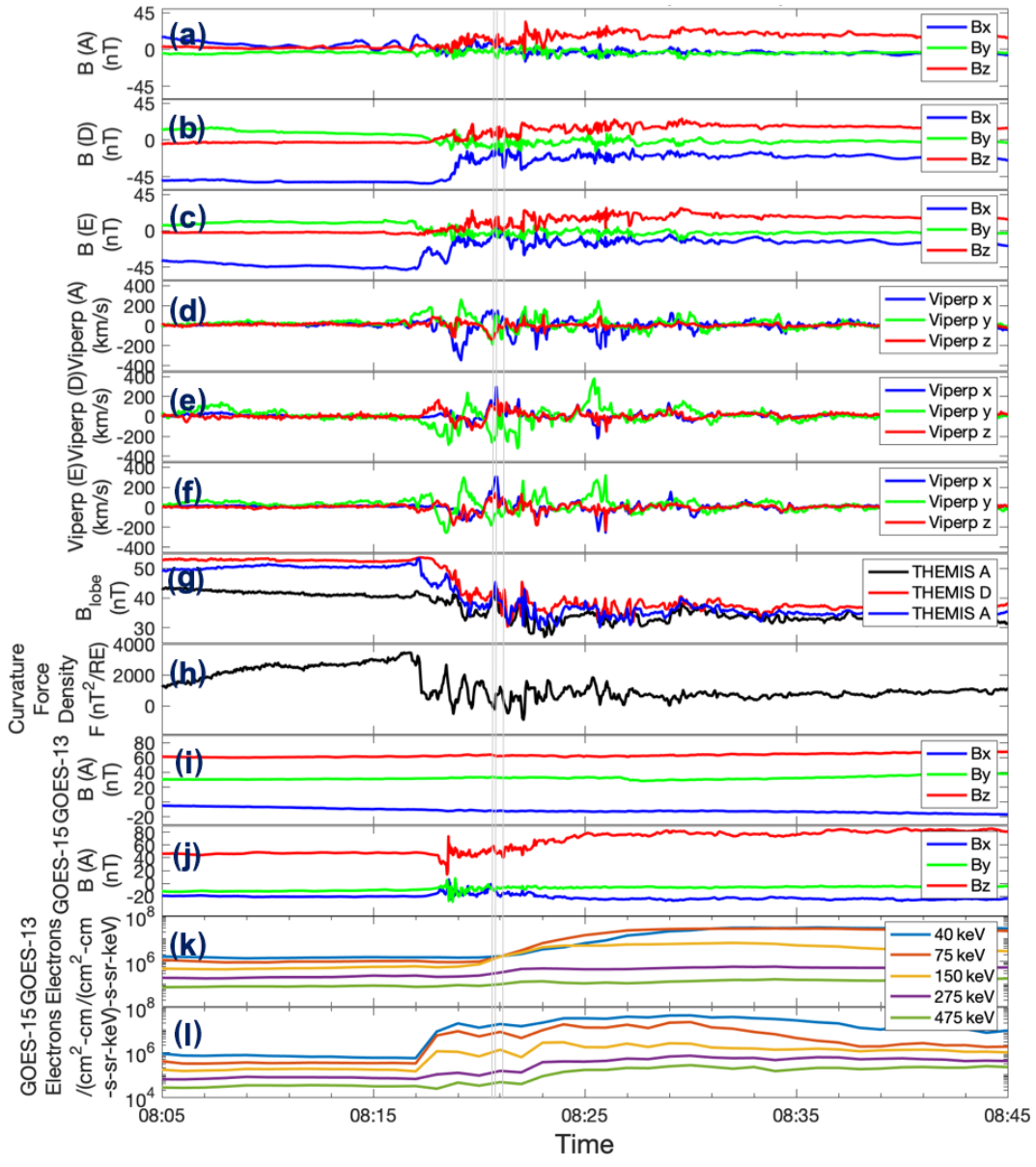

Figure 8. THEMIS and GOES in situ measurements for substorm fast flow burst Case 2 on 25 December 2015. The caption of Fig. 7 applies.

at 08:17 across all five energy channels (40, 75, 150, 275 and 475 keV), with the most significant increases in flux observed at low energies (e.g. 40, 75 and 150 keV), which were more pronounced (by up to 2 orders of magnitude). GOES 13 also observed an increase in flux across all energy channels a few minutes later despite being located more than 3 h MLT away on the dawn-side. This shows that substorm fast flow bursts are more likely to produce a strong inner magnetosphere response. The other two substorm fast flow bursts also show strong magnetosphere responses that were similarly observed by the GOES spacecraft. It is worth noting that we studied flux observations for other geosynchronous satellites that were ideally located on the nightside to observe such injections at the time of these fast flow bursts, such as the Los Alamos National Laboratory (LANL) satellites, for which similar particle injections were observed.

In addition, to understand the difference in the magnetospheric response between substorm fast flow bursts and pseudobreakups, we studied the curvature force density (F) (Li et al., 2011; Palin et al., 2012), estimated based on equatorial pressure gradient (Figs. 7h and 8h) and the magnetic lobe (B_{lobe}) (Figs. 7g and 8g), using the unique configuration of the three THEMIS spacecraft in close proximity and coplanar, with the normal directed along Y_{gsm} (Artemyev et al., 2019). The results show a clear and consistent difference between pseudobreakups and substorm fast flow

bursts. For pseudobreakups (Fig. 7), the B_{lobe} decreased from ~ 42 nT before the fast flow burst to ~ 34 nT after the fast flow burst, while there were fluctuations during the fast flow burst. The curvature force density also fluctuated, but was largely similar and relatively small before and after the fast flow burst ($\sim 50\,\mathrm{nT}^2\ {R_\mathrm{E}}^{-1}$). These observations are largely consistent for all three pseudobreakups, indicating that the pseudobreakups may not be able to penetrate deep into the inner magnetosphere (Dubyagin et al., 2011, 2010).

In contrast, for substorm fast flow bursts shown in Fig. 8, the decrease in B_{lobe} value was much more apparent as B_{lobe} decreased from ~ 54 to ~ 34 nT. Also, the fluctuations consisted of larger amplitudes and higher frequencies. The curvature force density increased gradually to $\sim 3400\,\mathrm{nT}^2\ {R_\mathrm{E}}^{-1}$ before the fast flow burst, which was much larger than what was observed for pseudobreakups (Fig. 7h). As energy is released during the fast flow burst, the curvature force density decreased to $\sim 800\,\mathrm{nT}^2\ {R_\mathrm{E}}^{-1}$ and remained relatively low, with large amplitude and high frequency fluctuations. These observations indicate that much more magnetic flux and energy (Chu et al., 2021) is released during substorm fast flow bursts than pseudobreakups and, hence, the substorm fast flow bursts are capable of penetrating deeper into the inner magnetosphere (Dubyagin et al., 2011, 2010). Figures and videos for all the cases that are not shown here are provided as supplementary material.

5 Conclusion

In this study, a multipoint analysis of conjugate magnetospheric and ionospheric observations was used to investigate the magnetospheric and ionospheric responses to substorm fast flow bursts and pseudobreakup events. The three inner THEMIS spacecraft's (THEMIS A, D and E) in situ measurements of THEMIS observations were used to select three pairs of fast flow bursts associated with substorm and pseudobreakup events. These fast flow bursts were observed during close separations on the nightside, beyond 6 R_E from the Earth in radial distance and a magnetic local time (MLT) region of ± 5 h from local midnight. The unique tail science phase configuration of the three THEMIS spacecraft provided the opportunity to study in detail the magnetospheric and ionospheric response to each substorm fast flow burst and pseudobreakup event, allowing us to derive time-varying parameters, such as the current density, lobe magnetic field, curvature force density and plasma pressure. Using these parameters, we were able to compare and understand what properties control the differences in the magnetosphere–ionosphere responses between substorm fast flow bursts and pseudobreakup events, and how these differences lead to different ionospheric responses.

The results show that ionospheric currents respond to both substorm fast flow bursts and pseudobreakup events. This indicates that the ionosphere currents are created by plasma flow vortices in the magnetosphere for fast flow bursts that are associated with substorms fast flow bursts and pseudobreakup events. The magnetic flux in the tail is much stronger for strong substorms and much weaker for pseudobreakup events. The B_{lobe} decreases significantly (by up to 40%) for substorm fast flow bursts, but is a much smaller decrease in B_{lobe} for pseudobreakup events. The curvature force density for pseudobreakups is much smaller than substorm fast flow events, indicating that the pseudobreakups may not be able to penetrate deep into the inner magnetosphere.

In addition, the magnetospheric and ionospheric response to substorm fast flow bursts is stronger compared to pseudobreakups. The pseudobreakups may only cause localised particle injections that do not penetrate very deep into the inner magnetosphere. However, more magnetic flux and energy are released during substorm fast flow bursts and, hence, substorm fast flow bursts are capable of penetrating deep into the inner magnetosphere and produce a much stronger magnetospheric response. This association can help us study the properties and activity of the magnetospheric earthward flow vortices from ground data. Satellite data are not always available to observe these events in the magnetosphere, whereas ground data can be readily available. Therefore, if we understand how these ionospheric currents respond to substorm fast flow bursts and pseudobreakup events, then we can determine magnetospheric conditions based on ground observations.

Data availability. The THEMIS data are publicly available at http://themis.ssl.berkeley.edu (Aryan, 2022a). The SECS-EIC data are publicly available at http://www.igpp.ucla.edu/public/jweygand/SECS/ (Aryan, 2022b). The GOES 13 and 15 electron flux data and magnetic field data are publicly available from NOAA (https://www.ngdc.noaa.gov/stp/satellite/goes/, Aryan, 2022c). We gratefully acknowledge the SuperMAG collaborators (https://supermag.jhuapl.edu/info/?page=acknowledgement). The SML, SMU and SME Indices (Newell and Gjerloev, 2011) were used in this study. The SuperMAG data are publicly available from http://supermag.jhuapl.edu/ (Aryan, 2022d).

Supplement. The supplement related to this article is available online at: https://doi.org/10.5194/angeo-40-531-2022-supplement.

Author contributions. HA was the lead author, contributed in gathering data, analysed the results and wrote the manuscript. JL contributed to the identification of fast flows and general discussions. JB contributed to data analysis and general discussion. JMW provided data of the ionospheric currents calculated using the SEC technique, helped with generating some of the figures and contributed to data analysis and general discussions. XC primarily provided the supermag data and contributed to data analysis and general discussions. VA is the THEMIS PI who helped with the THEMIS data and contributed to general discussion.

Competing interests. The contact author has declared that none of the authors has any competing interests.

Disclaimer. Publisher's note: Copernicus Publications remains neutral with regard to jurisdictional claims in published maps and institutional affiliations.

Acknowledgements. The authors would like to thank Anton Artemyev for useful discussions. Homayon Aryan, Jacob Bortnik, Jinxing Li, James Michael Weygand and Xiangning Chu would like to acknowledge the NASA HSR grant 80NSSC18K1227.

Financial support. This research has been supported by the National Aeronautics and Space Administration (grant no. 80NSSC18K1227).

Review statement. This paper was edited by Minna Palmroth and reviewed by two anonymous referees.

References

Akasofu, S.-I.: The Development of the Auroral Substorm, Planet. Space Sci., 12, 273–282, 1964.

Akasofu, S.-I.: Physics of Magnetospheric Substorms, D. Reidel, Dordrecht, the Netherlands, 170–187, 1976.

Amm, O. and Viljanen, A.: Ionospheric disturbance magnetic field continuation from the ground to the ionosphere using spherical elementary current systems, Earth Planets Space, 51, 431–440, https://doi.org/10.1186/BF03352247, 1999.

Amm, O., Engebretson, M. J., Hughes, T., Newitt, L., Viljanen, A., and Watermann, J.: A traveling convection vortex event study: Instantaneous ionospheric equivalent currents, estimation of field-aligned currents, and the role of induced currents, J. Geophys. Res.-Space, 107, SIA1-1–SIA1-11, https://doi.org/10.1029/2002JA009472, 2002.

Angelopoulos, V.: The THEMIS Mission, Space Sci. Rev., 141, 5, https://doi.org/10.1007/s11214-008-9336-1, 2008.

Angelopoulos, V., Baumjohann, W., Kennel, C. F., Coroniti, F. V., Kivelson, M. G., Pellat, R., Walker, R. J., Luehr, H., and Paschmann, G.: Bursty bulk flows in the inner central plasma sheet, J. Geophys. Res., 97, 4027–4039, 1992.

Angelopoulos, V., McFadden, J. P., Larson, D., Carlson, C. W., Mende, S. B., Frey, H., Phan, T., Sibeck, D. G., Glassmeier, K.-H., Auster, U., Donovan, E., Mann, I. R., Rae, I. J., Russell, C. T., Runov, A., Zhou, X.-Z., and Kepko, L.: Tail Reconnection Triggering Substorm Onset, Science, 321, 931–935, https://doi.org/10.1126/science.1160495, 2008.

Artemyev, A. V., Angelopoulos, V., Runov, A., and Petrukovich, A. A.: Global View of Current Sheet Thinning: Plasma Pressure Gradients and Large-Scale Currents, J. Geophys. Res.-Space, 124, 264–278, https://doi.org/10.1029/2018JA026113, 2019.

Aryan, H.: THEMIS data, http://themis.ssl.berkeley.edu, last access: 6 June 2022a.

Aryan, H.: SECs data, http://www.igpp.ucla.edu/public/jweygand/SECS/ , last access: 6 June 2022b.

Aryan, H.: GOES data, https://www.ngdc.noaa.gov/stp/satellite/goes/, last access: 6 June 2022c.

Aryan, H.: Supermag data, http://supermag.jhuapl.edu/, last access: 6 June 2022d.

Auster, H. U., Glassmeier, K. H., Magnes, W., Aydogar, O., Baumjohann, W., Constantinescu, D., Fischer, D., Fornacon, K. H., Georgescu, E., Harvey, P., Hillenmaier, O., Kroth, R., Ludlam, M., Narita, Y., Nakamura, R., Okrafka, K., Plaschke, F., Richter, I., Schwarzl, H., Stoll, B., Valavanoglou, A., and Wiedemann, M.: The THEMIS Fluxgate Magnetometer, Space Sci. Rev., 141, 235–264, https://doi.org/10.1007/s11214-008-9365-9, 2008.

Baker, D. N.: Solar wind-magnetosphere drivers of space weather, J. Atmos. Terr. Phys., 58, 1509–1526, 1996.

Baker, D. N., Fritz, T. A., Wilken, B., Higbie, P. R., Kaye, S. M., Kivelson, M. G., Moore, T. E., Stüdemann, W., Masley, A. J., Smith, P. H., and Vampola, A. L.: Observation and modeling of energetic particles at synchronous orbit on July 29, 1977, J. Geophys. Res.-Space, 87, 5917–5932, https://doi.org/10.1029/JA087iA08p05917, 1982.

Baumjohann, W., Paschmann, G., and Cattell, C. A.: Average plasma properties in the central plasma sheet, Geophys. Res. Lett., 94, 6597–6606, https://doi.org/10.1029/JA094iA06p06597, 1989.

Baumjohann, W., Blanc, M., Fedorov, A., and Glassmeier, K.-H.: Current Systems in Planetary Magnetospheres and Ionospheres, Space Sci. Rev., 152, 99–134, https://doi.org/10.1007/s11214-010-9629-z, 2010.

Birn, J. and Hesse, M.: The substorm current wedge in MHD simulations, J. Geophys. Res.-Space, 118, 3364–3376, https://doi.org/10.1002/jgra.50187, 2013.

Birn, J. and Hesse, M.: The substorm current wedge: Further insights from MHD simulations, J. Geophys. Res.-Space, 119, 3503–3513, https://doi.org/10.1002/2014JA019863, 2014.

Birn, J., Thomsen, M. F., Borovsky, J. E., Reeves, G. D., McComas, D. J., Belian, R. D., and Hesse, M.: Substorm ion injections: Geosynchronous observations and test particle orbits in three-dimensional dynamic MHD fields, J. Geophys. Res.-Space, 102, 2325–2341, https://doi.org/10.1029/96JA03032, 1997.

Birn, J., Nakamura, R., Panov, E. V., and Hesse, M.: Bursty bulk flows and dipolarization in MHD simulations of magnetotail reconnection, J. Geophys. Res.-Space, 116, A01210, https://doi.org/10.1029/2010JA016083, 2011.

Bonnell, J. W., Mozer, F. S., Delory, G., Hull, A. J., Ergun, R. E., Cully, C. M., V., A., and Harvey, P. R.: The electric field instrument (EFI) for THEMIS, Space Sci. Rev., 141, 303–341, 2008.

Borovsky, J. E. and Bonnell, J.: The dc electrical coupling of flow vortices and flow channels in the magnetosphere to the resistive ionosphere, J. Geophys. Res.-Space, 106, 28967–28994, https://doi.org/10.1029/1999JA000245, 2001.

Chu, X., McPherron, R. L., Hsu, T.-S., and Angelopoulos, V.: Solar cycle dependence of substorm occurrence and duration: Implications for onset, J. Geophys. Res.-Space, 120, 2808–2818, https://doi.org/10.1002/2015JA021104, 2015a.

Chu, X., McPherron, R. L., Hsu, T.-S., Angelopoulos, V., Pu, Z., Yao, Z., Zhang, H., and Connors, M.: Magnetic mapping effects of substorm currents leading to auroral poleward expansion

and equatorward retreat, J. Geophys. Res.-Space, 120, 253–265, https://doi.org/10.1002/2014JA020596, 2015b.

Chu, X., McPherron, R., Hsu, T., Angelopoulos, V., Weygand, J. M., Liu, J., and Bortnik, J.: Magnetotail flux accumulation leads to substorm current wedge formation: A case study, J. Geophys. Res.-Space, 126, https://doi.org/10.1029/2020JA028342, 2021.

Dubyagin, S., Sergeev, V., Apatenkov, S., Angelopoulos, V., Nakamura, R., McFadden, J., Larson, D., and Bonnell, J.: Pressure and entropy changes in the flow-braking region during magnetic field dipolarization, J. Geophys. Res.-Space, 115, A10225, https://doi.org/10.1029/2010JA015625, 2010.

Dubyagin, S., Sergeev, V., Apatenkov, S., Angelopoulos, V., Runov, A., Nakamura, R., Baumjohann, W., McFadden, J., and Larson, D.: Can flow bursts penetrate into the inner magnetosphere?, Geophys. Res. Lett., 38, L08102, https://doi.org/10.1029/2011GL047016, 2011.

Gabrielse, C., Spanswick, E., Artemyev, A., Nishimura, Y., Runov, A., Lyons, L., Angelopoulos, V., Turner, D. L., Reeves, G. D., McPherron, R., and Donovan, E.: Utilizing the Heliophysics/-Geospace System Observatory to Understand Particle Injections: Their Scale Sizes and Propagation Directions, J. Geophys. Res.-Space, 124, 5584–5609, https://doi.org/10.1029/2018JA025588, 2019.

Gjerloev, J. W.: A Global Ground-Based Magnetometer Initiative, EOS T. Am. Geophys. Un., 90, 230–231, https://doi.org/10.1029/2009EO270002, 2009.

Hones Jr., E. W., Akasofu, S.-I., Perreault, P., Bame, S. J., and Singer, S.: Poleward expansion of the auroral oval and associated phenomena in the magnetotail during auroral substorms: 1., J. Geophys. Res., 75, 7060–7074, https://doi.org/10.1029/JA075i034p07060, 1970.

Hsu, T. S. and McPherron, R. L.: A statistical analysis of substorm associated tail activity, Adv. Space Res.,, 50, 1317–1343, 2012.

Kauristie, K., Sergeev, V. A., Kubyshkina, M., Pulkkinen, T. I., Angelopoulos, V., Phan, T., Lin, R. P., and Slavin, J. A.: Ionospheric current signatures of transient plasma sheet flows, J. Geophys. Res.-Space, 105, 10677–10690, https://doi.org/10.1029/1999JA900487, 2000.

Keiling, A., Angelopoulos, V., Runov, A., Weygand, J., Apatenkov, S. V., Mende, S., McFadden, J., Larson, D., Amm, O., Glassmeier, K.-H., and Auster, H. U.: Substorm current wedge driven by plasma flow vortices: THEMIS observations, J. Geophys. Res.-Space, 114, A00C22, https://doi.org/10.1029/2009JA014114, 2009.

Kepko, L., McPherron, R. L., Amm, O., Apatenkov, S., W., B., Birn, J., Lester, M., Nakamura, R., Pulkkinen, T. I., and Sergeev, V.: Substorm Current Wedge Revisited, Space Sci. Rev., 190, 1–46, 2014.

Kepko, L., McPherron, R. L., Amm, O., Apatenkov, S., Baumjohann, W., Birn, J., Lester, M., Nakamura, R., Pulkkinen, T. I., and Sergeev, V.: Substorm Current Wedge Revisited, Space Sci. Rev., 190, 1–46, https://doi.org/10.1007/s11214-014-0124-9, 2015.

Koskinen, H. E. J., Lopez, R. E., Pellinen, R. J., Pulkkinen, T. I., Baker, D. N., and Bösinger, T.: Pseudobreakup and substorm growth phase in the ionosphere and magnetosphere, J. Geophys. Res.-Space, 98, 5801–5813, https://doi.org/10.1029/92JA02482, 1993.

Li, J., Chu, X., Bortnik, J., Weygand, J., Wang, C.-P., Liu, J., McPherron, R., and Kellerman, A.: Characteristics of Substorm-Onset-Related and Non-substorm Earthward Fast Flows and Associated Magnetic Flux Transport: THEMIS Observations, J. Geophys. Res.-Space, 126, e2020JA028313, https://doi.org/10.1029/2020JA028313, 2021.

Li, S.-S., Angelopoulos, V., Runov, A., Zhou, X.-Z., McFadden, J., Larson, D., Bonnell, J., and Auster, U.: On the force balance around dipolarization fronts within bursty bulk flows, J. Geophys. Res.-Space, 116, A00I35, https://doi.org/10.1029/2010JA015884, 2011.

Liu, J., Angelopoulos, V., Runov, A., and Zhou, X.-Z.: On the current sheets surrounding dipolarizing flux bundles in the magnetotail: The case for wedgelets, J. Geophys. Res.-Space, 118, 2000–2020, https://doi.org/10.1002/jgra.50092, 2013a.

Liu, J., Angelopoulos, V., Zhou, X.-Z., Runov, A., and Yao, Z.: On the role of pressure and flow perturbations around dipolarizing flux bundles, J. Geophys. Res.-Space, 118, 7104–7118, https://doi.org/10.1002/2013JA019256, 2013b.

Liu, J., Angelopoulos, V., Zhou, X.-Z., and Runov, A.: Magnetic flux transport by dipolarizing flux bundles, J. Geophys. Res.-Space, 119, 909–926, https://doi.org/10.1002/2013JA019395, 2014.

Liu, J., Angelopoulos, V., Chu, X., Zhou, X.-Z., and Yue, C.: Substorm current wedge composition by wedgelets, Geophys. Res. Lett., 42, 1669–1676, https://doi.org/10.1002/2015GL063289, 2015.

Lopez, R. E., Sibeck, D. G., McEntire, R. W., and Krimigis, S. M.: The energetic ion substorm injection boundary, J. Geophys. Res.-Space, 95, 109–117, https://doi.org/10.1029/JA095iA01p00109, 1990.

Lyons, L. R., Nishimura, Y., Xing, X., Runov, A., Angelopoulos, V., Donovan, E., and Kikuchi, T.: Coupling of dipolarization front flow bursts to substorm expansion phase phenomena within the magnetosphere and ionosphere, J. Geophys. Res.-Space, 117, A02212, https://doi.org/10.1029/2011JA017265, 2012.

McIlwain, C. E.: Plasma convection in the vicinity of the geosynchronous orbit, 269, Springer Dordrecht, Dordrecht, the Netherlands, 1972.

McPherron, R. L.: Growth phase of magnetospheric substorms, J. Geophys. Res. (1896–1977), 75, 5592–5599, https://doi.org/10.1029/JA075i028p05592, 1970.

McPherron, R. L.: Magnetospheric substorms, Rev. Geophys., 17, 657–681, https://doi.org/10.1029/RG017i004p00657, 1979.

McPherron, R. L. and Chu, X.: The Mid-Latitude Positive Bay and the MPB Index of Substorm Activity, Space Sci. Rev., 206, 91–122, https://doi.org/10.1007/s11214-016-0316-6, 2017.

McPherron, R. L. and Chu, X.: The Midlatitude Positive Bay Index and the Statistics of Substorm Occurrence, J. Geophys. Res.-Space, 123, 2831–2850, https://doi.org/10.1002/2017JA024766, 2018.

McPherron, R. L., Russell, C. T., and Aubry, M. P.: Satellite studies of magnetospheric substorms on August 15, 1968: 9. Phenomenological model for substorms, J. Geophys. Res. (1896–1977), 78, 3131–3149, https://doi.org/10.1029/JA078i016p03131, 1973.

McPherron, R. L., Hsu, T.-S., Kissinger, J., Chu, X., and Angelopoulos, V.: Characteristics of plasma flows at the inner edge of the plasma sheet, J. Geophys. Res.-Space, 116, A00I33, https://doi.org/10.1029/2010JA015923, 2011.

Nakamura, R., Baker, D. N., Yamamoto, T., Belian, R. D., Bering III, E. A., Benbrook, J. R., and Theall, J. R.: Particle and field signatures during pseudobreakup and major expansion onset, J. Geophys. Res.-Space, 99, 207–221, https://doi.org/10.1029/93JA02207, 1994.

Nakamura, R., Baumjohann, W., Schödel, R., Brittnacher, M., Sergeev, V. A., Kubyshkina, M., Mukai, T., and Liou, K.: Earthward flow bursts, auroral streamers, and small expansions, J. Geophys. Res.-Space, 106, 10791–10802, https://doi.org/10.1029/2000JA000306, 2001.

Nakamura, R., Baumjohann, W., Klecker, B., Bogdanova, Y., Balogh, A., Rème, H., Bosqued, J. M., Dandouras, I., Sauvaud, J. A., Glassmeier, K.-H., Kistler, L., Mouikis, C., Zhang, T. L., Eichelberger, H., and Runov, A.: Motion of the dipolarization front during a flow burst event observed by Cluster, Geophys. Res. Lett., 29, 3-1–3-4, https://doi.org/10.1029/2002GL015763, 2002.

Nakamura, R., Baumjohann, W., Mouikis, C., Kistler, L. M., Runov, A., Volwerk, M., Asano, Y., Vörös, Z., Zhang, T. L., Klecker, B., Rème, H., and Balogh, A.: Spatial scale of high-speed flows in the plasma sheet observed by Cluster, Geophys. Res. Lett., 31, L09804, https://doi.org/10.1029/2004GL019558, 2004.

Nakamura, R., Retinò, A., Baumjohann, W., Volwerk, M., Erkaev, N., Klecker, B., Lucek, E. A., Dandouras, I., André, M., and Khotyaintsev, Y.: Evolution of dipolarization in the near-Earth current sheet induced by Earthward rapid flux transport, Ann. Geophys., 27, 1743–1754, https://doi.org/10.5194/angeo-27-1743-2009, 2009.

Newell, P. T. and Gjerloev, J. W.: Evaluation of SuperMAG auroral electrojet indices as indicators of substorms and auroral power, J. Geophys. Res.-Space, 116, A12211, https://doi.org/10.1029/2011JA016779, 2011.

Nishimura, Y., Lyons, L. R., Angelopoulos, V., Kikuchi, T., Zou, S., and Mende, S. B.: Relations between multiple auroral streamers, pre-onset thin arc formation, and substorm auroral onset, J. Geophys. Res.-Space, 116, A09214, https://doi.org/10.1029/2011JA016768, 2011.

Ohtani, S., Anderson, B. J., Sibeck, D. G., Newell, P. T., Zanetti, L. J., Potemra, T. A., Takahashi, K., Lopez, R. E., Angelopoulos, V., Nakamura, R., Klumpar, D. M., and Russell, C. T.: A multisatellite study of a pseudo-substorm onset in the near-Earth magnetotail, J. Geophys. Res.-Space, 98, 19355–19367, https://doi.org/10.1029/93JA01421, 1993.

Palin, L., Jacquey, C., Sauvaud, J.-A., Lavraud, B., Budnik, E., Angelopoulos, V., Auster, U., McFadden, J. P., and Larson, D.: Statistical analysis of dipolarizations using spacecraft closely separated along Z in the near-Earth magnetotail, J. Geophys. Res.-Space, 117, A09215, https://doi.org/10.1029/2012JA017532, 2012.

Rowland, W. and Weigel, R. S.: Intracalibration of particle detectors on a three-axis stabilized geostationary platform, Space Weather, 10, S11002, https://doi.org/10.1029/2012SW000816, 2012.

Runov, A., Sergeev, V. A., Angelopoulos, V., Glassmeier, K.-H., and Singer, H. J.: Diamagnetic oscillations ahead of stopped dipolarization fronts, J. Geophys. Res.-Space, 119, 1643–1657, https://doi.org/10.1002/2013JA019384, 2014.

Runov, A., Angelopoulos, V., Gabrielse, C., Liu, J., Turner, D. L., and Zhou, X.-Z.: Average thermodynamic and spectral properties of plasma in and around dipolarizing flux bundles, J. Geophys. Res.-Space, 120, 4369–4383, https://doi.org/10.1002/2015JA021166, 2015.

Sergeev, V., Nishimura, Y., Kubyshkina, M., Angelopoulos, V., Nakamura, R., and Singer, H.: Magnetospheric location of the equatorward prebreakup arc, J. Geophys. Res.-Space, 117, A01212, https://doi.org/10.1029/2011JA017154, 2012.

Sergeev, V. A., Chernyaev, I. A., Angelopoulos, V., Runov, A. V., and Nakamura, R.: Stopping flow bursts and their role in the generation of the substorm current wedge, Geophys. Res. Lett., 41, 1106–1112, https://doi.org/10.1002/2014GL059309, 2014.

Sibeck, D. G. and Angelopoulos, V.: THEMIS Science Objectives and Mission Phases, Space Sci. Rev., 141, 35–59, https://doi.org/10.1007/s11214-008-9393-5, 2008.

Sitnov, M. I., Buzulukova, N., Swisdak, M., Merkin, V. G., and Moore, T. E.: Spontaneous formation of dipolarization fronts and reconnection onset in the magnetotail, Geophys. Res. Lett., 40, 22–27, https://doi.org/10.1029/2012GL054701, 2013.

Sun, W. J., Fu, S. Y., Parks, G. K., Liu, J., Yao, Z. H., Shi, Q. Q., Zong, Q.-G., Huang, S. Y., Pu, Z. Y., and Xiao, T.: Field-aligned currents associated with dipolarization fronts, Geophys. Res. Lett., 40, 4503–4508, https://doi.org/10.1002/grl.50902, 2013.

Weygand, J. M. and Wing, S.: Comparison of DMSP and SECS region-1 and region-2 ionospheric current boundary, J. Atmos. Sol.-Terr. Phys., 143–144, 8–13, https://doi.org/10.1016/j.jastp.2016.03.002, 2016.

Weygand, J. M., Amm, O., Viljanen, A., Angelopoulos, V., Murr, D., Engebretson, M. J., Gleisner, H., and Mann, I.: Application and validation of the spherical elementary currents systems technique for deriving ionospheric equivalent currents with the North American and Greenland ground magnetometer arrays, J. Geophys. Res.-Space, 116, A03305, https://doi.org/10.1029/2010JA016177, 2011.

Weygand, J. M., Amm, O., Angelopoulos, V., Milan, S. E., Grocott, A., Gleisner, H., and Stolle, C.: Comparison between SuperDARN flow vectors and equivalent ionospheric currents from ground magnetometer arrays, J. Geophys. Res.-Space, 117, A05325, https://doi.org/10.1029/2011JA017407, 2012.

Yao, Z. H., Pu, Z. Y., Fu, S. Y., Angelopoulos, V., Kubyshkina, M., Xing, X., Lyons, L., Nishimura, Y., Xie, L., Wang, X. G., Xiao, C. J., Cao, X., Liu, J., Zhang, H., Nowada, M., Zong, Q. G., Guo, R. L., Zhong, J., and Li, J. X.: Mechanism of substorm current wedge formation: THEMIS observations, Geophys. Res. Lett., 39, L13102, https://doi.org/10.1029/2012GL052055, 2012.